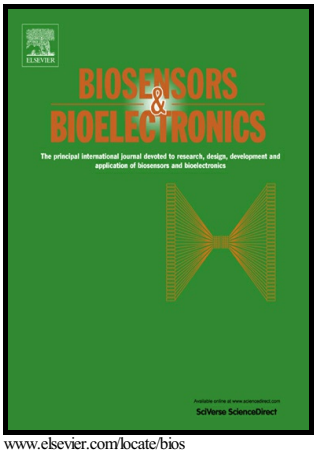

www.elsevier.com/locate/bios

A Novel Capacitive Sensor Based on Molecularly Imprinted Nanoparticles as Recognition Elements

Francesco Canfarotta, Joanna Czulak, Antonio Guerreiro, Alvaro Garcia Cruz, Sergey Piletsky, Gizem Ertürk Bergdahl, Martin Hedström, Bo Mattiasson

PII: S0956-5663(18)30580-3
DOI: https://doi.org/10.1016/j.bios.2018.07.070
Reference: BIOS10659

To appear in: *Biosensors and Bioelectronic*

Received date: 11 May 2018
Revised date: 27 July 2018
Accepted date: 30 July 2018

Cite this article as: Francesco Canfarotta, Joanna Czulak, Antonio Guerreiro, Alvaro Garcia Cruz, Sergey Piletsky, Gizem Ertürk Bergdahl, Martin Hedström and Bo Mattiasson, A Novel Capacitive Sensor Based on Molecularly Imprinted Nanoparticles as Recognition Elements, *Biosensors and Bioelectronic,* https://doi.org/10.1016/j.bios.2018.07.070

A Novel Capacitive Sensor Based on Molecularly Imprinted Nanoparticles as Recognition Elements

Francesco Canfarotta [1], Joanna Czulak [1], Antonio Guerreiro [1*], Alvaro Garcia Cruz[2], Sergey Piletsky[2], Gizem Ertürk Bergdahl[3,4], Martin Hedström[4,5], Bo Mattiasson[4,5]

[1]MIP Diagnostics Ltd., Fielding Johnson Building, University of Leicester, LE1 7RH, United Kingdom

[2]Chemistry Department, University of Leicester, LE1 7RH, United Kingdom

[3]Department of Clinical Sciences, Division of Infection Medicine, Biomedical Center B14, Lund University, SE-221 84 Lund, Sweden

[4]CapSenze Biosystems AB, Scheelevägen 22, SE-223 63 Lund, Sweden

[5]Department of Biotechnology, Lund University, Naturvetarvägen 14, SE-221 00 Lund, Sweden

[*]Corresponding author, email: ag@mip-dx.com

ABSTRACT

Molecularly Imprinted Polymers (MIPs) are synthetic receptors capable of selective binding to their target (template) molecules and, hence, are used as recognition elements in assays and sensors as a replacement for relatively unstable enzymes and antibodies. Herein, we describe a manufacturing-friendly protocol for integration of MIP nanoparticles (nanoMIPs) with a (label-free) capacitive sensor. The nanoMIPs were produced by solid-phase synthesis for two templates with different sizes and properties, including a small molecule tetrahydrocannabinol (THC) and a protein (trypsin). NanoMIPs were deposited on the surface of the sensor and the change in capacitance (ΔC) upon binding of the target was measured. The significant improvement in the selectivity and limit of detection (one order of magnitude compared to previously used MIP microparticles) can be attributed to their increased surface-to-volume ratio and higher specificity of the nanoMIPs produced by the solid-phase method. The methodology described is also compatible with common sensor fabrication approaches, as opposed to methods involving in situ MIP polymerisation. The proposed sensor shows high selectivity, fast sensor response (45 min including injection, regeneration and re-equilibration with running buffer), and straightforward data analysis, which makes it viable for label-free

monitoring *in real-time.* The set of targets assessed in this manuscript shows the general applicability of the biosensor platform.

Keywords: MIP; biosensor; capacitance; protein sensor; nanoparticle

1. INTRODUCTION

Molecularly Imprinted Polymers (MIPs) are synthetic receptors capable of selective binding to target (template) molecules. This is due to the presence of highly specific recognition sites that are complementary to the template in terms of size, shape, and orientation of functional groups (Sellergren and Allender, 2005; Whitcombe et al., 2014; Wulff, 2002)[1-3]. The major technological progress achieved in MIP technology in the last ten years include: development of generic protocol for polymer design using computational approaches (Cowen et al., 2016), and production of high performance MIPs capable of operating in aqueous environment (Piletska et al., 2008) . Two remaining principal issues that must be addressed before we would see commercial success of MIPs in diagnostic applications are: lack of protocols for integration MIPs with optical and electrochemical detectors, compatible with mass-manufacturing of sensor devices, and lack or reliable approach for transforming MIP-template interactions into detectable electrical signal. Bulk monoliths have been the most common MIP format, however, even after grinding, this process typically produces microparticles which are not suitable for incorporation in sensors. MIPs prepared in nano-sized format (nanoMIPs) are better suited for integration with sensing devices (Haupt and Mosbach, 2000). In general nanoMIPs hold great potential in theranostics and implantable sensors also in light of their good biocompatibility (Canfarotta et al., 2016a, 2016b). The most advanced protocol for production of MIP nanoparticles with pseudo-monoclonal properties is solid-phase synthesis (Canfarotta et al., 2016a). Currently, nanoMIPs produced by solid-phase synthesis are applied as recognition elements in assays, optical and electrochemical sensors (Altintas et al., 2015; Basozabal et al., 2014; Caceres et al., 2016; Canfarotta et al., 2017; Chianella et al., 2013; Korposh et al., 2014; Smolinska-Kempisty et al., 2017, 2016; Tang et al., 2017). The use of these synthetic binders presents several advantages over their natural counterparts, such as cost-effectiveness of polymer preparation, simple and scalable synthesis, and robustness (Mahony et al., 2005; Ye and Haupt, 2004). MIPs in general can operate in harsh environments such as under extremes of

pH, temperature and also in organic solvents (Kriz and Mosbach, 1995; Svenson and Nicholls, 2001). Their robustness makes nanoMIPs viable for use in remote geographical areas where cold chain might be unavailable.

Although the use of MIPs for extraction of target molecules in complex matrices is quite widespread, their application in practical sensors remains comparatively limited. As mentioned above, this can be explained by the inherent difficulty to incorporate bulk/film MIPs into sensor platforms and, also, by the lack of transduction methods that allow a straightforward and fast analysis (Huang et al., 2007; Turner, 2000). These limitations can be overcome by separating the nanoMIP preparation step from sensor fabrication. This way the nanoMIP can be used to reproducibly prepare sensors by techniques already in place (e.g. screen-printing, spin and deep-coating, printing etc.), such as those developed for sensor fabrication using antibodies. Also, this allows for separate quality control of the nanoMIP solution, which can then be deposited as any other off-the-shelf bio-affinity reagent. The practical option is to combine such nanoMIPs with capacitance sensors that do not require electrochemical labels and can be used for detection of neutral and charged species. The general principle of capacitive measurements is based on the displacement of the counter ions around the gold capacitive electrode when a target (analyte) binds to the receptor on polymer-electrode interface which results in a change in capacitance. As the amount of target molecules binding on the sensor surface increases, the achieved displacement and the decrease in the total capacitance will increase too (Lebogang et al., 2014). The system enables highly sensitive and selective detection in a label-free fashion, thus without requiring any additional reagents for signal amplification (Ertürk et al., 2015; Ertürk and Lood, 2018; Ertürk and Mattiasson, 2017). The main advantages of capacitive sensors are their high sensitivity, label-free measurement, low power consumption, easy detection, low cost and flexibility in choosing sensor size and reduction in required sample volume (Ertürk et al., 2016a).

In previous works, we have demonstrated that capacitive biosensors offer higher sensitivity as compared with other techniques. Ertürk et al. developed a capacitive biosensor system for prostate specific antigen (PSA) detection where they achieved a limit of detection (LOD) of 8.0×10^{-5} ng mL^{-1} (16×10^{-17} M) (Ertürk et al., 2015). Subsequently, the same authors developed a surface plasmon resonance (SPR) biosensor for PSA in order to compare the detection performances of two systems, and they found a LOD of 91 pg mL^{-1} (18×10^{-14} M) for the SPR method (Ertürk et al., 2016b). The capacitive system was almost 1000 times more

sensitive than the SPR system. In a similar comparison, Idil et al. developed a capacitive biosensor for *E. coli* detection by using a microcontact imprinting method, where they reported a LOD value of 70 CFU mL^{-1} (Idil et al., 2017). On the other hand, Yilmaz et al. used the same microcontact imprinting method to develop a SPR and QCM biosensor for *E. coli* detection, in which they reported LOD values of 1.54×10^6 CFU mL^{-1} and 3.72×10^5 CFU/mL for SPR and QCM systems respectively (Yilmaz et al., 2015). Even in this case, the capacitive biosensor achieved a sensitivity almost 100 times higher than SPR and QCM systems.

In this work, we developed nanoMIPs for two targets that differ in molecular weight, a small molecule (tetrahydrocannabinol – THC) and a protein (trypsin). Herein we demonstrate that we can measure these molecules at physiologically relevant concentrations with our proposed capacitive sensor. The developed sensor holds great potential in diagnostics due to its sensitivity, simplicity to operate, rapid and low-cost detection. As nanoMIPs can be produced against virtually any target, this sensor platform can be extended to other biomolecules by simply varying the nanoMIPs.

2. MATERIALS AND METHODS

2.1. Materials

Tyramine, tetrahydrocannabinol (THC), 11-nor-9-carboxytetrahydrocannabinol, cannabidivarin, acrylic acid (AA), acrylamide (AAm) *N*-isopropylacrylamide (NIPAm) *N*,*N*-methylene-bis-acrylamide (BIS), *N*-tert-butylacrylamide (TBAm), ammonium persulfate (APS), trypsin, tetramethylethylenediamine (TEMED), *N*-[3-(trimethoxysilyl)propyl]ethylenediamine, *N*-ethyldiisopropylamine (EIPA), sodium hydroxide (NaOH), ethylene glycol dimethacrylate (EGDMA), trimethylolpropane trimethacrylate (TRIM), pentaerythritol tetrakis(3-mercaptopropionate) (PETMP), dimethylformamide (DMF), *N*,*N*-diethyldithiocarbamic acid benzyl ester (INIFERTER), *N*-(3-Aminopropyl)methacrylamide hydrochloride (NAPMA), (3-glycidyloxypropyl)trimetoxysilane (GOPTS), glutaraldehyde, 50% solution in water, (GA), acetone, 1-ethyl-3-(3-dimethylaminopropyl)-carbodiimide hydrochloride (EDC), *N*-hydroxysuccinimide (NHS) and [3-(2-aminoethylamino)propyl]trimethoxysilane (APTMS) were purchased from Sigma-Aldrich, UK. Phosphate buffered saline (PBS) pH 7.4 was prepared, as specified, from PBS buffer tablets (Sigma-Aldrich, UK) and consisted of phosphate buffer (0.01 M), potassium chloride (0.0027 M), and sodium chloride (0.137 M). 1-Dodecanethiol was obtained from Aldrich (Deisenhofen, Germany). Glass beads (Spheriglass 2429 CP00,

53-106 μm diameter) were purchased from Blagden Chemicals, UK. In all experiments double-distilled ultrapure (DI) water was used. All chemicals and solvents were of analytical or HPLC grade and used without further purification.

2.2 Methods

2.1.1 Preparation of template-modified glass beads (solid-phase functionalization)

Glass beads were first activated by boiling in a 2 M NaOH solution for 15 min, then washed with deionized water and rinsed with acetone, dried at 80 °C.

For trypsin immobilisation, activated glass beads were incubated overnight in 2 % v/v APTMS in a dry toluene solution (0.4 mL solution per g glass beads). Subsequently APTMS-derivatised glass beads were incubated in a 7% (v/v) GA solution in PBS for 2 h. Afterwards, the beads were washed with 700 mL of distilled water and placed in a bottle containing trypsin (0.1 mg mL^{-1}) in PBS, and incubated overnight at 4 °C. After overnight incubation, the beads were washed with 500 mL of water in a sintered funnel and used for the synthesis of nanoMIPs.

For the preparation of THC-modified solid-phase, 60 g of activated glass beads were placed in a solution of 3% GOPTS and 2 mg mL^{-1} EIPA in anhydrous toluene solution at 70°C for 24 h. Subsequently, the glass beads were filtered and washed with acetone and dried. For THC immobilization, dry beads were incubated in a 0.5 mg mL^{-1} THC solution in a 1:9 mixture water/acetonitrile at pH 10 for 24 h. Then, glass beads were washed with acetonitrile, double-distilled water and then dried.

2.1.2 Synthesis of THC and trypsin-imprinted nanoMIPs

The procedure was adapted from Canfarotta et al., 2016a. For the synthesis of trypsin nanoMIPs, the following monomers were dissolved in distilled water (100 ml): NIPAM (39 mg), BIS (6 mg), TBAm (33 mg), NAPMA (5.8 mg), AA (2.2 μL). TBAm was previously dissolved in ethanol (1 mL) and then added to the aqueous solution. The solution containing the monomers was degassed under vacuum and sonicated for 5 min, and then purged with N_2 for 20 min. Then, 60 g of template-derivatised glass beads were added to the solution. Polymerisation was initiated by adding ammonium persulfate aqueous solution (800 μL, 60 mg mL^{-1}) and TEMED (24 μL). The headspace was flushed with N_2 and the bottle sealed with a screw cap. Polymerisation was carried-out at room temperature for 1 h. Subsequently, the content of the polymerisation

vessel was poured into a solid-phase extraction cartridge (60 mL) equipped with a frit (20 µm porosity). A total of 9 washes with 20 mL of distilled water at 20°C was carried out to remove low affinity nanoMIPs, oligomers and unreacted monomer. Afterwards, the SPE cartridge containing the solid-phase was placed in a water bath at 70°C for 15 min. An aliquot of 20 mL of distilled water pre-warmed at 65 °C was poured into the SPE to collect the high-affinity nanoMIPs. This procedure was repeated seven times, until about 140 mL of a solution of high-affinity nanoMIPs in water was collected.

For the synthesis of THC-imprinted nanoMIPs, 30g of THC-modified beads were added to a previously degassed polymerisation mixture (10 min with bubbling N_2), which consisted of 1.29 g BIS, 3.24 g EGDMA, 3.24 g TRIM, 0.112 g NAPMA, 1.19 g AAm, 0.18 g of PETMP and 0.75 g of INIFERTER in 25 mL of DMF as solvent. The polymerisation was accomplished under UV radiation (1 min and 30 sec).

Unreacted monomers were removed by washing 3 times with 10 mL of cold DMF (4°C) and 5 times with 10 mL of cold ACN (4°C). High affinity nanoMIPs were collected by washing 10 times with 10 mL hot ACN (65°C).

To ensure complete removal of all unreacted monomer from the bulk of the nanoparticles, aliquots of the collected solution were concentrated down to 2 ml using a centrifugal dialysis cartridge fitted with a membrane with 30 kDa molecular weight cut-off (Amicon Ultra, Merck Millipore) to remove unreacted monomers and other side products. This was followed by seven washes (14 mL) with deionized water on the same dialysis cartridge.

2.1.3 Size and concentration analysis of nanoMIPs

The particle size was measured with a Zetasizer Nano (Nano-S) particle-size analyser from Malvern Instruments Ltd (UK). An aliquot of the dispersion of nanoMIPs in distilled water was sonicated for 2 min and then analysed by DLS at 25 °C in a 3 mL disposable polystyrene cuvette. The instrument automatically chose attenuator position, measurement duration and number of runs. The values are reported as an average of 4 measurements. Transmission Electron Microscopy (TEM) images of nanoMIPs were taken using a JEOL JEM 1010, 100 kV high contrast TEM equipped with a Gatan SC1000 Orius CCD camera (Gatan, Abingdon Oxon, UK). Samples for the analysis have been prepared by depositing a drop of the nanoMIPs dispersion, previously filtered through a 1.2 µm porosity PES syringe filter, on a carbon-coated TEM copper

grid (400 mesh), and leaving them to dry at room temperature. The nanoMIP concentration was assessed by freeze-drying an aliquot (20 ml) of the particle solution and then weighing the solid.

2.1.4 Preparation of immobilized nanoMIPs capacitive biosensor electrodes

In the first step, the electrodes were cleaned with ethanol, de-ionized water, acetone, de-ionized water and acidic Piranha solution (3:1, H_2SO_4:H_2O_2, V/V) respectively for 10 min in each step. Then electro-polymerisation of tyramine was performed by cyclic voltammetry (CV) in ethanolic solution of 10 mM tyramine with a set potential range of 0–1.5 V (vs Ag/AgCl) and a scan rate of 50 mV s^{-1} for 15 scans. By doing so, free primary amino groups were introduced on the surface of the electrode. Then the electrodes were rinsed with distilled water and dried with nitrogen gas.

In the second step, the electrodes were immersed in 5.0% (v/v) glutaraldehyde in 25 mM sodium phosphate buffer (pH 7.4) for 1 h at room temperature. Then, they were thoroughly rinsed with phosphate buffer and dried with nitrogen gas. This way, the amino groups on the surface of the electrode are modified by coupling to one of the aldehyde groups of glutaraldehyde leaving one free aldehyde group.

Finally, the electrodes were incubated in a nanoMIPs solution (0.06 mg mL^{-1}) prepared in 25 mM phosphate buffer (pH 7.4) overnight at 4°C. Then, the electrodes were immersed in 1-dodecanethiol (10 mM) in ethanol for 20 min in order to cover bare parts of the gold surface. To visualise the immobilised nanoMIPs, the THC nanoMIP electrode was characterised by AFM using a Veeco Dimension 3100 Scanning Probe Microscope (Veeco Instruments Inc. USA), operating NanoScope 6.12 Software. Tapping mode was selected, using a Tap300 antimony-doped silicon probe tip (Bruker, UK) with a scan area size of 10.0 × 10.0 μm.

The THC nanoMIP electrode was also characterized by Cyclic Voltammetry (Ivium Compactstat, Netherlands) in order to determine the insulation level of the electrodes. All electrochemical measurements were conducted in a standard three-electrode flow cell fitted with a platinum wire and a commercial Ag/AgCl electrodes as the reference and counter electrodes, respectively. THC nanoMIPs electrode was used as the working electrode. A solution of KCl (0.1 M) containing 0.1 M potassium ferricyanide was used as the electrolyte solution. CV experiments were performed by sweeping the potential between -0.3 and 0.8 V at a sweep rate of 0.1 V s^{-1}.

2.1.5 Capacitive measurements with immobilized nanoMIPs

The capacitive measurements were performed by using current pulse method, as described in previous articles (Analytica Chimica Acta, 2015, 891: 120-129).(Sensors and Actuators B: Chemical, 2014, 190: 295-304) .

The theory for the current pulse technique is based on the principle of an electrical double layer and the electrode solution interface is based on an assumption that the system could be described as a simple resistor–capacitor (RC) circuit model. Generally for the capacitive biosensor assay, the electrode is modified with an insulating layer. Hence, an accurate description of the electrode interface would be an R(RC) circuit. As the electrode surface is insulated, the ohmic resistance (RF) of the insulating layer is much higher than the electrical resistance of the element serially connected to the layer (RS). This high RF simulates an open circuit and the system could thus be simplified as RC circuit having an extra resistor (R) serially connected to a capacitor (C). When the RC circuit is charged by a constant current, I, the potential (U) increases linearly with time (t). The potential response can be simultaneously sampled from the potential curve that is built up across the sensor when it is charged with a constant current. The electrical resistance (R) is calculated by using Ohms law (Equation 1).

$$U = I \times R \qquad \text{(Equation 1)}$$

where U is the voltage when time is zero and I is the applied current. The capacitance is then calculated from the slope of the potential curve through equation 2.

$$C = (I \times t) / U \qquad \text{(Equation 2)}$$

where I is the current supplied to the sensor, t is the current pulse period and U is the slope of the voltage built up across the capacitor of the RC circuit multiplied with time. The evaluated capacitances (nF) are then plotted against time (min).

Capacitive measurements were performed in a continuous flow system with an automated capacitance measuring device as shown in Figure 1. In the first step, a regeneration solution (25 mM glycine-HCl, pH 2.5) was injected into the system to regenerate the surface. This step was repeated between each analyte injection. After injection of running buffer to get a stable baseline, standard solutions of different concentrations of the template (analyte) were injected sequentially with regeneration and reconditioning in

between. The binding of the target protein (trypsin) to the electrode surface resulted in a decrease of the registered capacitance and the change was calculated automatically by CapSenze Smart Software (CSS). In all of the analyses, the flow rate was 100 µL min^{-1} and the injected sample volume was 250 µL.

In order to evaluate the selectivity of the immobilized nanoMIPs sensors, the responses of the capacitive sensor against competitor molecules were monitored. These analyses were carried out for trypsin and THC with the corresponding nanoMIPs immobilized on the electrodes.

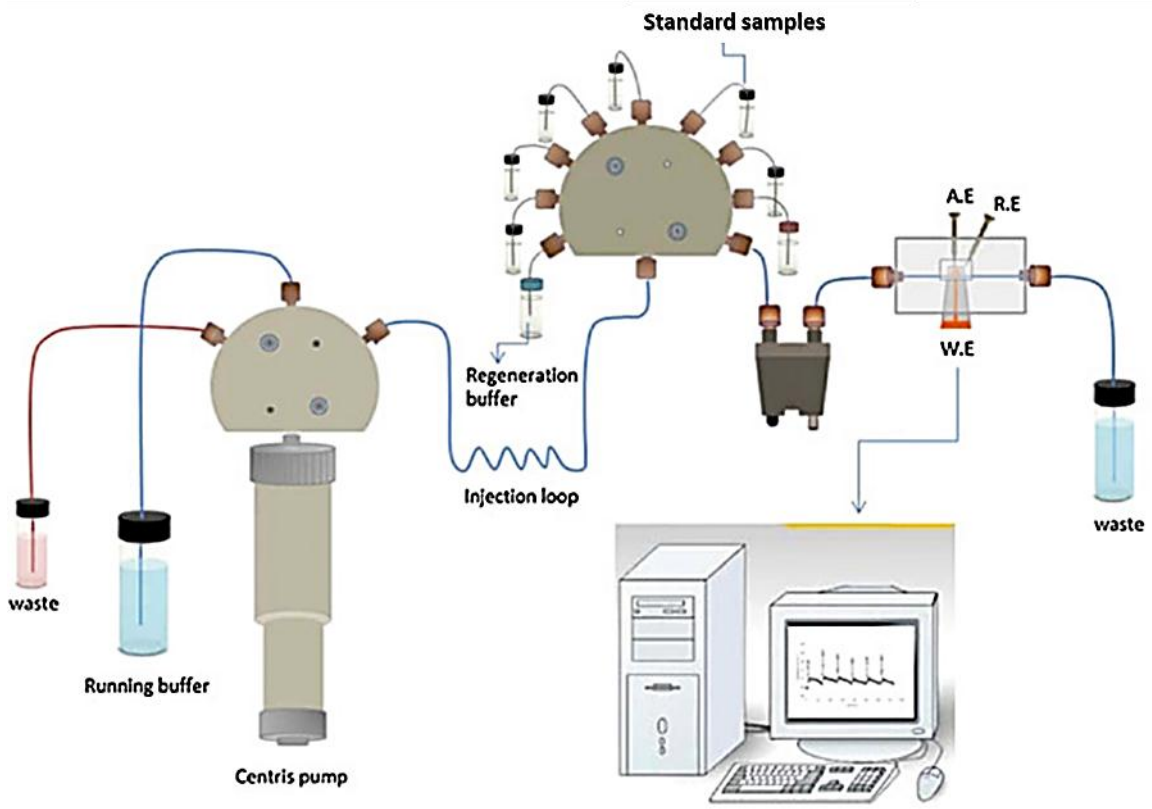

Figure 1. Schematic diagram showing the capacitive sensor with an automated flow injection system, reproduced from (Ertürk et al., 2014).

3. RESULTS and DISCUSSION

3.1. Production and characterization of nanoMIPs

Herein we assess whether molecularly imprinted nanoparticles (nanoMIPs) can act as recognition elements in a capacitive sensor, and whether they can improve the LOD and specificity of such sensors. The innovative solid-phase approach used to produce nanoMIPs relies on the covalent immobilisation of the template molecule on a solid support (in this example, glass beads with average diameter of 90 µm). The

polymerisation is then performed in the presence of such a support bearing the immobilised template. After polymerisation, the solid support acts as an affinity medium to isolate the high-affinity nanoMIPs from the remaining monomers, oligomers and low-affinity polymers (Figure 2). Thanks to this affinity purification step, obtained nanoMIPs possess high affinity and specificity toward their targets and exhibit a more homogeneous distribution of binding site affinities compared to nanoMIPs produced in solution (i.e. without solid-phase or affinity puriffication) (Chianella et al., 2013). Furthermore, as previously demonstrated, such solid-phase approach allows for the production of nanoMIPs virtually free from template (since the latter is covalently immobilised on the support) and in a short time-frame (2-3 hours). Moreover, this approach can be easily automated to allow the production of nanoMIPs with improved batch-to-batch consistency and reduced user intervention (Poma et al., 2013). It is worth mentioning that nanoMIPs produced by this solid-phase approach were successfully used to target specific peptides also *in vivo*, thus demonstrating their potential in diagnostics and performance in complex matrixes (Cecchini et al., 2017).

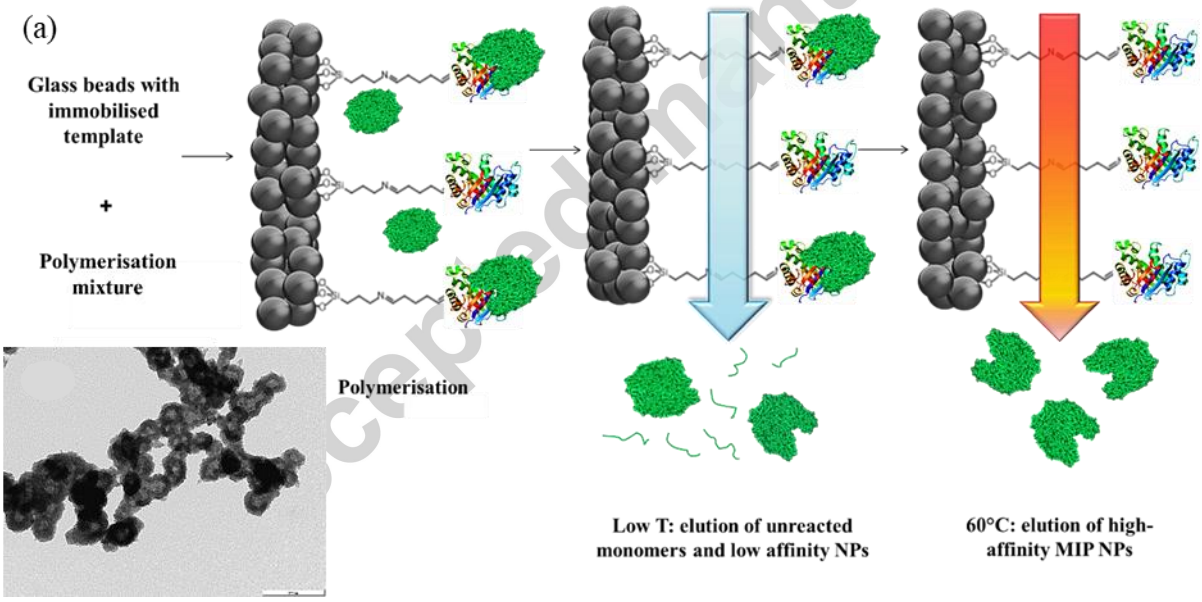

Figure 2. Scheme of the solid-phase synthesis of nanoMIPs. In this example, a protein is shown as the template molecule, inset shows a TEM image of THC MIPs. Scale bar 200 nm.

NanoMIPs against THC and trypsin were produced, therefore covering a range of template sizes and showing the general applicability of the method. It is worth mentioning that, to date, nanosized MIP structures have not been used in combination with capacitance detection. AFM measurements of the

electrode surface before and after nanoMIP shows presence of additional surface features with an approximate diameter of 100 nm distributed throughout but not covering totally the available surface, see SI.

The hydrodynamic size of the two types of nanoMIPs was determined by DLS in water (Table 1). It should be noted that the hydrodynamic size can differ from the dry size obtained from TEM for several reasons: first, most nanosystems typically undergo a certain level of agglomeration in solution, which leads to an apparent increase in their size by DLS; secondly, the polymer tends to hydrate and swell when in solution. Also, smaller particles scatter less light than larger particles (intensity of the scattering proportional to the sixth power of the particle diameter), and therefore shifting the measured size to higher values.

Table 1. Hydrodynamic size of the four different nanoMIPs by DLS in distilled water.

Target	Size (nm)	PDI
THC	168 ± 8	0.29
Trypsin	320 ± 7	0.22

3.2. Capacitive measurements

The capacitance value measured on the electrode surface is built up by the contribution of different layers according to equation 3 below:

$$\frac{1}{C\,(total)} = \frac{1}{C\,(ins)} + \frac{1}{C\,(bio)} + \frac{1}{C\,(dl)} \qquad \text{(Equation 3)}$$

According to this equation, total change in capacitance is the sum of capacitance contributions from insulating, biosensing and diffuse layers, respectively. As shown in the Figure S 1 (See SI), the degree of insulation increased after immobilization of nanoMIPs and this last step reduced the redox currents substantially. This result shows that the surface of the electrode is insulated well enough to be used in the subsequent capacitive measurements. Binding of the target molecule to the receptor on the biosensing layer creates a displacement of the counter ions (diffuse layer) around the gold surface and a decrease in the total capacitance. Therefore, the more target molecules bind to the receptor, the higher the decrease in total capacitance (Ctot) will be. This forms the general principle of capacitive measurements as shown on a sensorgram in Figure 3.

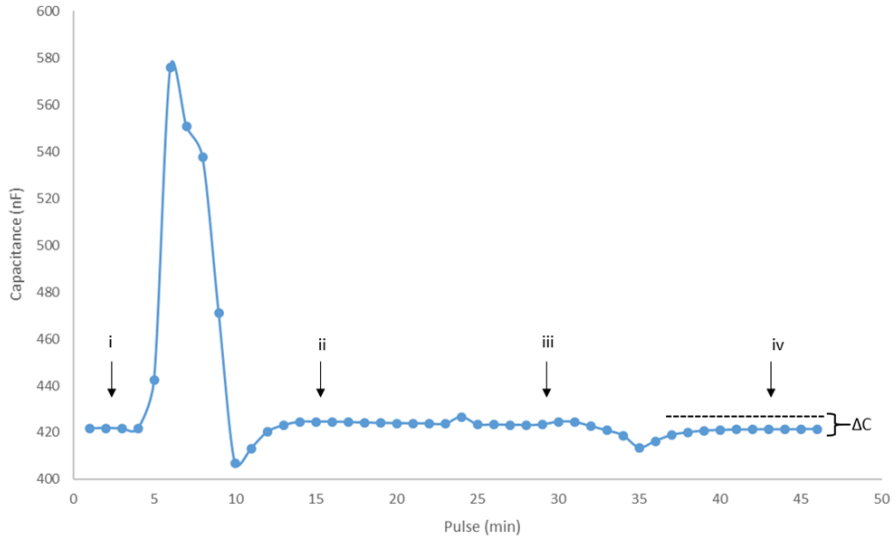

Figure 3. Target analyte (THC) binding to the gold electrode (THC concentration: 10^{-5} M) . Actual sensorgram showing the real-time binding of target analyte on the immobilized nanoMIPS gold electrode. Numbered phrases represent: (i) stable baseline before regeneration, (ii) stable baseline after regeneration and re-equilibration of the system just before injection, (iii) injection of the target analyte, (iv) binding of the target analyte causing a decrease in the capacitance (ΔC = change in capacitance after target analyte binding to the surface).

Standard analyte solutions were prepared in running buffer (10 mM phosphate, pH: 7.4) and injected sequentially into the system. The dynamic concentration ranges were 1.0 x 10^{-14} – 1.0 x 10^{-9} M for trypsin and 1.0 x 10^{-12} – 1.0 x 10^{-5} M for THC. The calibration graphs (Figure 4) show the capacitance change vs. log concentration of two target analytes. Such capacitance changes showed a linear relationship for both targets. Limit of detection (LOD) values were calculated as 1.0 x 10^{-14} M for trypsin and 1.0 x 10^{-14} M for THC. These results show that templates/analytes with different sizes can be detected in a broad concentration range with high sensitivities.

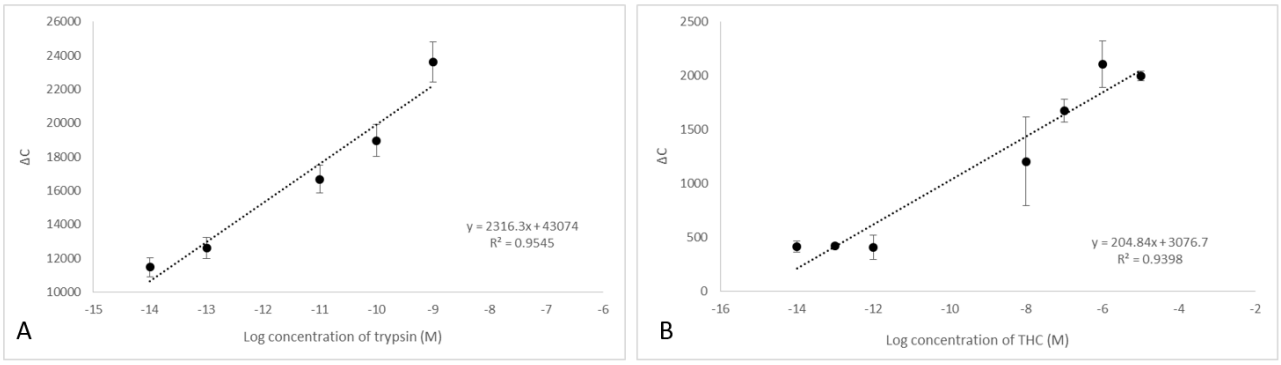

Figure 4. Calibration curves showing the capacitance vs (A) trypsin and (B) THC concentrations in optimum conditions (ΔC: -pF.cm^{-2}, Running buffer: 10 mM phosphate, pH: 7.4; Regeneration Buffer: 25 mM glycine-HCl, pH: 2.5; Flow rate: 100 µL.min^{-1}, Sample volume: 250 µL).

In order to demonstrate the selectivity of the immobilized nanoMIPs, different compounds were injected into the system and the sensor responses for these competitor molecules were compared with the responses for template analytes. The results are shown in Figure 5. The sensor response for other molecules was significantly low in all occasions. Preferential binding of the target molecules was observed over related analogues. The calculated selectivity coefficients are shown in Table 2. Selectivity coefficients (k) are calculated by using the equation 4:

$$k = \frac{\Delta Ctarget}{\Delta Ccompetitor} \qquad \text{(Equation 4)}$$

This high selectivity of the system shows that the nanoMIPs are highly selective for their targets and can be successfully integrated within the proposed sensor systems for label free selective detection of analytes.

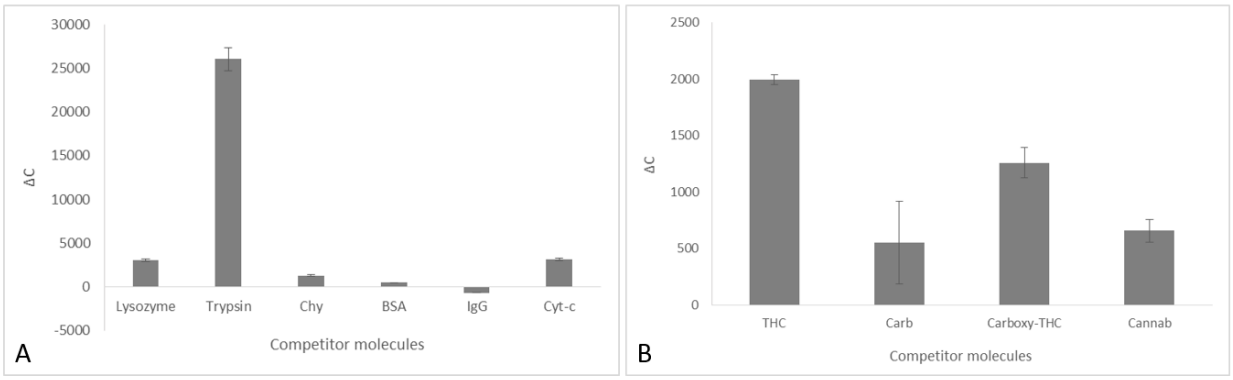

Figure 5. Selectivity of immobilized (A) trypsin and (B) THC nanoMIPs capacitive sensors vs. competitor molecules in optimum conditions (Concentration of all the compounds: 0.1 mg.mL^{-1}, ΔC: -pF.cm^{-}2, Running buffer: 10 mM

phosphate, pH: 7.4; Regeneration Buffer: 25 mM glycine-HCl, pH: 2.5; Flow rate: 100 μL.min^{-1}, Sample volume: 250 μL).

Table 2. Selectivity coefficients of immobilized (A) trypsin and (B) THC nanoMIPS capacitive sensors [ΔC; -pF.cm^{-2}: change in capacitance value upon binding of an analye, k: selectivity coefficient].

Analyte (A)	**ΔC**	**k**
Trypsin	26023	-
Chymotrypsin	1295	20.1
Lysosyme	3046	8.5
BSA	481	54.1
Cyt-c	3139	8.3
Analyte (B)		
THC	1996	-
Cannabidivarin	552	3.62
11-nor-9-carboxy-Δ^9-THC	1259	1.59
Cannabigerol	658	3.03

4. Conclusions

MIP nanoparticles produced with a solid-phase approach were imprinted against two analytes with different molecular weights (THC and trypsin). The solid support was used as a medium to isolate the high affinity nanoMIPs from the low affinity particles. A homogeneous distribution of particles (in the range of 161-320 nm, depending on the target molecule) was obtained, which was confirmed by TEM analysis and DLS. Subsequently, the nanoMIPs were used to functionalise sensor chips. Capacitive tests demonstrated that the nanoMIPs can be successfully employed as selective capturing agents for detection of a range of analytes with different properties (charge, molecular weight, polarity). This demonstrates the general applicability of this sensor combined with nanoMIPs as recognition elements. LoDs are obtained in the low nanomolar range, with an evident enhancement of selectivity over other contaminants, compared with previous works in which MIPs were used in similar sensor platform (Ertürk et al., 2016a). This is attributed to the use of nanoMIPs, which are pre-selected during the solid-phase preparation process to have high affinity binding sites.

The high sensitivity of capacitive biosensors combined with the high selectivity of nanoMIPs can be promising in various applications where a sensitive, selective and label-free detection is required. The use of this capacitance-based approach in combination with the nanoMIP technology can offer sensors that are able

to detect biomolecules in a simple, cost-effective (around £8 per electrode, which can also be regenerated several times) and in a fast (<5 min) manner. The stability of the MIPs enables the use of the sensor electrodes repeatedly, even under rough conditions which was reported in the previous articles (Ertürk et al. 2016a, 2016b; 2014). In this study, prepared electrodes were used more than 70 assays during a period of 2 months with good reproducibility without any significant loss in the activity. Finally, the described methodology is versatile and can be tailored to the intended application by varying the nanoMIP receptor.

References

Altintas, Z., Gittens, M., Guerreiro, A., Thompson, K.-A., Walker, J., Piletsky, S., Tothill, I.E., 2015. Detection of Waterborne Viruses Using High Affinity Molecularly Imprinted Polymers. Anal. Chem. 87, 6801–6807. https://doi.org/10.1021/acs.analchem.5b00989

Basozabal, I., Guerreiro, A., Gomez-Caballero, A., Aranzazu Goicolea, M., Barrio, R.J., 2014. Direct potentiometric quantification of histamine using solid-phase imprinted nanoparticles as recognition elements. Biosens. Bioelectron. 58, 138—144. https://doi.org/10.1016/j.bios.2014.02.054

Caceres, C., Canfarotta, F., Chianella, I., Pereira, E., Moczko, E., Esen, C., Guerreiro, A., Piletska, E., Whitcombe, M.J., Piletsky, S.A., 2016. Does size matter? Study of performance of pseudo-ELISAs based on molecularly imprinted polymer nanoparticles prepared for analytes of different sizes. Analyst 141, 1405–1412. https://doi.org/10.1039/C5AN02018B

Canfarotta, F., Poma, A., Guerreiro, A., Piletsky, S., 2016. Solid-phase synthesis of molecularly imprinted nanoparticles. Nat. Protoc. 11, 443–455.

Canfarotta, F., Smolinska-Kempisty, K., Piletsky, S.A., 2017. Replacement of Antibodies in Pseudo-ELISAs: Molecularly Imprinted Nanoparticles for Vancomycin Detection., in: Methods in Molecular Biology. pp. 389–398.

Canfarotta, F., Waters, A., Sadler, R., McGill, P., Guerreiro, A., Papkovsky, D., Haupt, K., Piletsky, S., 2016b. Biocompatibility and internalization of molecularly imprinted nanoparticles. Nano Res. 9, 3463–3477. https://doi.org/10.1007/s12274-016-1222-7

Cecchini, A., Raffa, V., Canfarotta, F., Signore, G., Piletsky, S., MacDonald, M.P., Cuschieri, A., 2017. In Vivo Recognition of Human Vascular Endothelial Growth Factor by Molecularly Imprinted

Polymers. Nano Lett. 17, 2307–2312. https://doi.org/10.1021/acs.nanolett.6b05052

Chianella, I., Guerreiro, A., Moczko, E., Caygill, J.S., Piletska, E. V, Perez De Vargas Sansalvador, I.M., Whitcombe, M.J., Piletsky, S.A., 2013. Direct replacement of antibodies with molecularly imprinted polymer (MIP) nanoparticles in ELISA – development of a novel assay for vancomycin. Anal. Chem. https://doi.org/10.1021/ac402102j

Cowen, T., Karim, K., Piletsky, S., 2016. Computational approaches in the design of synthetic receptors – A review. Anal. Chim. Acta 936, 62–74. https://doi.org/https://doi.org/10.1016/j.aca.2016.07.027

Ertürk, G., Berillo, D., Hedström, M., Mattiasson, B., 2014. Microcontact-BSA imprinted capacitive biosensor for real-time, sensitive and selective detection of BSA. Biotechnol. Rep 3, 65–72. https://doi.org/https://doi.org/10.1016/j.btre.2014.06.006

Ertürk, G., Hedström, M., Mattiasson, B., 2016a. A sensitive and real-time assay of trypsin by using molecular imprinting-based capacitive biosensor. Biosens. Bioelectron. 86, 557–565. https://doi.org/https://doi.org/10.1016/j.bios.2016.07.046

Ertürk, G., Hedström, M., Tümer, M.A., Denizli, A., Mattiasson, B., 2015. Real-time prostate-specific antigen detection with prostate-specific antigen imprinted capacitive biosensors. Anal. Chim. Acta 891, 120–129. https://doi.org/10.1016/j.aca.2015.07.055

Ertürk, G., Lood, R., 2018. Bacteriophages as biorecognition elements in capacitive biosensors: Phage and host bacteria detection. Sens. Actuators B Chem. 258, 535–543. https://doi.org/https://doi.org/10.1016/j.snb.2017.11.117

Ertürk, G., Mattiasson, B., 2017. Capacitive Biosensors and Molecularly Imprinted Electrodes. Sensors, 17, 390. https://doi.org/10.3390/s17020390

Ertürk, G., Özen, H., Tümer, M.A., Mattiasson, B., Denizli, A., 2016b. Microcontact imprinting based surface plasmon resonance (SPR) biosensor for real-time and ultrasensitive detection of prostate specific antigen (PSA) from clinical samples. Sensors Actuators B Chem. 224, 823–832. https://doi.org/https://doi.org/10.1016/j.snb.2015.10.093

Haupt, K., Mosbach, K., 2000. Molecularly Imprinted Polymers and Their Use in Biomimetic Sensors. Chem. Rev. 100, 2495–2504. https://doi.org/10.1021/cr990099w

Huang, C.-Y., Syu, M.-J., Chang, Y.-S., Chang, C.-H., Chou, T.-C., Liu, B.-D., 2007. A portable potentiostat for the bilirubin-specific sensor prepared from molecular imprinting. Biosens. Bioelectron. 22, 1694–1699. https://doi.org/https://doi.org/10.1016/j.bios.2006.07.036

Idil, N., Hedström, M., Denizli, A., Mattiasson, B., 2017. Whole cell based microcontact imprinted capacitive biosensor for the detection of Escherichia coli. Biosens. Bioelectron. 87, 807–815. https://doi.org/https://doi.org/10.1016/j.bios.2016.08.096

Korposh, S., Chianella, I., Guerreiro, A., Caygill, S., Piletsky, S., James, S.W., Tatam, R.P., 2014. Selective vancomycin detection using optical fibre long period gratings functionalised with molecularly imprinted polymer nanoparticles. https://doi.org/10.1039/c3an02126b

Kriz, D., Mosbach, K., 1995. Competitive amperometric morphine sensor based on an agarose immobilised molecularly imprinted polymer. Anal. Chim. Acta 300, 71–75. https://doi.org/https://doi.org/10.1016/0003-2670(94)00368-V

Lebogang, L., Mattiasson, B., Hedström, M., 2014. Capacitive sensing of microcystin variants of Microcystis aeruginosa using a gold immunoelectrode modified with antibodies, gold nanoparticles and polytyramine. Microchim. Acta 181, 1009–1017. https://doi.org/10.1007/s00604-014-1199-4

Mahony, J.O., Nolan, K., Smyth, M.R., Mizaikoff, B., 2005. Molecularly imprinted polymers—potential and challenges in analytical chemistry. Anal. Chim. Acta 534, 31–39. https://doi.org/https://doi.org/10.1016/j.aca.2004.07.043

Piletska, E. V, Guerreiro, A.R., Romero-Guerra, M., Chianella, I., Turner, A.P.F., Piletsky, S.A., 2008. Design of molecular imprinted polymers compatible with aqueous environment. Anal. Chim. Acta 607, 54–60. https://doi.org/10.1016/j.aca.2007.11.019

Poma, A., Guerreiro, A., Whitcombe, M.J., Piletska, E. V, Turner, A.P.F., Piletsky, S.A., 2013. Solid-Phase Synthesis of Molecularly Imprinted Polymer Nanoparticles with a Reusable Template–"Plastic Antibodies." Adv. Funct. Mater. 23, 2821–2827. https://doi.org/10.1002/adfm.201202397

Sellergren, B., Allender, C.J., 2005. Molecularly imprinted polymers: A bridge to advanced drug delivery. Adv. Drug Deliv. Rev. 57, 1733–1741. https://doi.org/https://doi.org/10.1016/j.addr.2005.07.010

Smolinska-Kempisty, K., Ahmad, O.S., Guerreiro, A., Karim, K., Piletska, E., Piletsky, S., 2017. New

potentiometric sensor based on molecularly imprinted nanoparticles for cocaine detection. Biosens. Bioelectron. 96, 49–54. https://doi.org/https://doi.org/10.1016/j.bios.2017.04.034

Smolinska-Kempisty, K., Guerreiro, A., Canfarotta, F., Cáceres, C., Whitcombe, M.J., Piletsky, S., 2016. A comparison of the performance of molecularly imprinted polymer nanoparticles for small molecule targets and antibodies in the ELISA format 6, 37638.

Svenson, J., Nicholls, I.A., 2001. On the thermal and chemical stability of molecularly imprinted polymers. Anal. Chim. Acta 435, 19–24. https://doi.org/https://doi.org/10.1016/S0003-2670(00)01396-9

Tang, S.-P., Canfarotta, F., Smolinska-Kempisty, K., Piletska, E., Guerreiro, A., Piletsky, S., 2017. A pseudo-ELISA based on molecularly imprinted nanoparticles for detection of gentamicin in real samples. Anal. Methods 9, 2853–2858. https://doi.org/10.1039/C7AY00398F

Turner, A.P.F., 2000. Biosensors--Sense and Sensitivity. Science (80-.). 290, 1315 LP-1317.

Whitcombe, M.J., Kirsch, N., Nicholls, I., 2014. Molecular imprinting science and technology: a survey of the literature for the years 2004–2011. J. Mol. Recognit. 27, 297–401. https://doi.org/10.1002/jmr.2347

Wulff, G., 2002. Enzyme-like Catalysis by Molecularly Imprinted Polymers. Chem. Rev. 102, 1–28. https://doi.org/10.1021/cr980039a

Ye, L., Haupt, K., 2004. Molecularly imprinted polymers as antibody and receptor mimics for assays, sensors and drug discovery. Anal. Bioanal. Chem. 378, 1887–1897. https://doi.org/10.1007/s00216-003-2450-8

Yilmaz, E., Majidi, D., Ozgur, E., Denizli, A., 2015. Whole cell imprinting based Escherichia coli sensors: A study for SPR and QCM. Sensors Actuators B Chem. 209, 714–721. https://doi.org/https://doi.org/10.1016/j.snb.2014.12.032

Highlights

- Molecularly imprinted nanoparticles were integrated with a capacitance sensor
- Methodology used for sensor fabrication is compatible with existing approaches
- Sensors showed high selectivity, fast responses and were reusable